Robust colonoscope tracking method for colon deformations utilizing coarse-to-fine correspondence findings

**Masahiro Oda · Hiroaki Kondo ·
Takayuki Kitasaka · Kazuhiro Furukawa ·
Ryoji Miyahara · Yoshiki Hirooka ·
Hidemi Goto · Nassir Navab · Kensaku
Mori**

Abstract *Purpose* Polyps found during CT colonography can be removed by
colonoscopic polypectomy. A colonoscope navigation system that navigates a
physician to polyp positions while performing the colonoscopic polypectomy is
required. Colonoscope-tracking methods are essential for implementing colono-
scope navigation systems. Previous colonoscope-tracking methods have failed
when the colon deforms during colonoscope insertions. This paper proposes a
colonoscope-tracking method that is robust against colon deformations.

M. Oda · H. Kondo
Graduate School of Information Science, Nagoya University,
Furo-cho, Chikusa-ku, Nagoya, Aichi, Japan
Tel.: +81-(0)52-789-5688
Fax: +81-(0)52-789-3815
E-mail: moda@mori.m.is.nagoya-u.ac.jp

T. Kitasaka
School of Information Science, Aichi Institute of Technology,
1247 Yachigusa, Yagusa-cho, Toyota, Aichi, Japan

K. Furukawa · R. Miyahara · H. Goto
Nagoya University Graduate School of Medicine,
65 Tsurumai-cho, Syouwa-ku, Nagoya, Aichi, Japan

Y. Hirooka
Department of Endoscopy, Nagoya University Hospital,
65 Tsurumai-cho, Syouwa-ku, Nagoya, Aichi, Japan

N. Navab
Technische Universität München,
Boltzmannstr. 3, 85748 Garching bei München, Germany

K. Mori
Information and Communications, Nagoya University,
Furo-cho, Chikusa-ku, Nagoya, Aichi, Japan

Method The proposed method generates a colon centerline from a CT volume and a curved line representing the colonoscope shape (colonoscope line) by using electromagnetic sensors. We find correspondences between points on a deformed colon centerline and colonoscope line by a landmark-based coarse correspondence finding and a length-based fine correspondence finding processes. Even if the coarse correspondence finding process fails to find some correspondences, which occurs with colon deformations, the fine correspondence finding process is able to find correct correspondences by using previously recorded line lengths.

Result Experimental results using a colon phantom showed that the proposed method finds the colonoscope-tip position with tracking errors smaller than 50 mm in most trials. A physician who specializes in gastroenterology commented that tracking errors smaller than 50 mm are acceptable. This is because polyps are observable from the colonoscope camera when positions of the colonoscope-tip and polyps are closer than 50 mm.

Conclusions We developed a colonoscope-tracking method that is robust against deformations of the colon. Because the process was designed to consider colon deformations, the proposed method can track the colonoscope-tip position even if the colon deforms.

Keywords Colon · Colonoscope tracking · CT image · EM sensor

1 Introduction

Computed tomographic colonography (CTC), or virtual colonoscopy, has recently received attention as a new colon diagnostic method [1]. It utilizes computed tomographic (CT) volumes of a patient to diagnose the colon. CTC is applicable as a screening test for detecting colonic polyps [2]. Computer-aided diagnosis (CAD) systems for CTC are commercially available. Such systems help physicians to observe the inside of the colon and to find suspicious regions, including colonic polyps. In CAD systems for CTC, physicians explore the inside of the colon using 2D, 3D, or virtual unfolded views of the colon. Colonic polyps can be found by using automated colonic polyp detection methods. CAD systems for CTC have information about colon shapes and colonic polyp positions.

If colonic polyps or early-stage cancers are found by CTC CAD, a patient is given a colonoscopic examination or colonoscopic polypectomy to perform further diagnosis and polyp removal. A colonoscopic polypectomy is the removal of a colonic polyp. Colonic-polyp removal in the early stage reduces the risk of development of colon cancers. While performing a colonoscopic examination, a physician controls the colonoscope based on colonoscopic images. The colonoscopic images only show views from the colonoscope-tip. A physician has to estimate how the colonoscope is traveling inside the colon based on experience. However, position estimation is difficult because the colon and colonoscope have long and winding shapes. The colon changes shape significantly during colonoscope insertion. Some inexperienced physicians cause com-

plications such as colon perforation during examinations. If the colon has an abnormal shape, controlling the colonoscope is difficult even for experienced physicians. Such problems are caused by misestimation of the positions and shapes of the colon and colonoscope by physicians. One way to prevent such problems is to introduce a navigation system for colonoscope examination. A colonoscope-tracking method that estimates the position and shape of the colonoscope in the colon is an essential function for colonoscope-navigation systems.

Tracking methods of endoscopes have been proposed by several research groups [3–11]. For bronchoscope tracking, image-based or sensor-based methods have been proposed [3–10]. Image-based bronchoscope tracking methods estimate camera positions and movements based on 2D/3D image registrations. To estimate camera positions and movements, some methods make correspondences between temporally continuous bronchoscopic images based on feature points to implement [3]. Correspondences between bronchoscopic images and virtualized bronchoscopic images are also utilized for tracking [4–6]. Sensor-based tracking methods utilize small position and direction sensors attached to a bronchoscope [7,8]. Combined techniques of image- and sensor-based tracking are also reported[9,10]. Since the trachea and bronchi deform due to breathing motion, most of the bronchoscope tracking methods try to compensate for the breathing motion. For colonoscope tracking, an image-based method has been proposed [11]. They estimate colonoscope camera movements from optical flows of colonoscopic images. However, they tracked camera movements only for the parts of colonoscopic videos where video images were clear. In colonoscopic examinations, unclear colonoscopic images are frequently obtained due to fluid, feces, and bubbles in the colon. Furthermore, the colon changes shape significantly during colonoscope insertions. Image-based tracking methods are difficult to track for long periods. Sensor-based methods are also developed to guide colonoscope insertions [12, 13]. These methods just calculate the colonoscope path. They cannot estimate the colonoscope position in the colon.

We propose a new colonoscope-tracking method that utilizes a colon deformation robust coarse-to-fine line registration technique. Our method tackles the difficulty of colon tracking that is caused by colon deformations. The colon shape in a CT volume and the shape of the colonoscope in the colon are represented as curved lines. Their shapes are quite different because of the colon deformations. The proposed method make correspondences between the curved lines using the coarse-to-fine correspondence finding process. The correspondence finding is tolerant to correspondence loses caused in coarse step. Such correspondence loses occur many times during a colonoscope insertion because of large deformations of the colon. The tolerance of the correspondence finding is achieved by recovering correspondences utilizing line length history data. The colonoscope-tip position in the colon is estimated based on the calculated correspondences. The coarse-to-fine correspondence finding makes our method robust against deformations of the colon occur by colonoscope insertions. Our method use electromagnetic (EM) sensors to obtain colonoscope

position and shapes. Therefore, our method can track the colonoscope-tip regardless of colonoscopic image quality. Most of the processes in our method are automated to reduce manual interactions. Furthermore, our method estimates colonoscope-tip position in real time. Advantages of the proposed method can be summarized as: (1) robust for colon deformations by accepting some correspondence loses, (2) unaffected by colonoscopic image quality, (3) minimal manual operations, and (4) real time tracking.

Preliminary reports about this paper have been published in conference proceedings [14–16]. In these reports, a landmark-based coarse correspondence finding and a length-based fine correspondence finding processes were utilized. The landmark-based coarse correspondence finding process failed to make correspondences when the colon largely deforms by colonoscope insertions. The length-based fine correspondence finding fails in such situation. Large difference between the colon centerline and colonoscope line was not considered in the preliminary reports. This paper presents an extended method to stably perform colonoscope tracking in situations where significant deformations of the colon or colonoscope occur. In this paper, the length-based fine correspondence finding use current and previously recorded line lengths to estimate the colonoscope-tip position. When the landmark-based coarse correspondence finding fails to make correspondences, subsequently performed length-based fine correspondence finding use previously recorded line length to estimate the colonoscope-tip position. This enables continuous colonoscope-tip position tracking even if the colon largely deforms during colonoscope insertions.

2 Method

2.1 Overview

Our colonoscope-tracking method calculates a position in the colon in a CT volume that corresponds to a colonoscope-tip position in the patient body. A CT volume of a patient and outputs of EM sensors attached to a colonoscope are used. Figure 1 shows a flowchart of the proposed method.

The colonoscope-tracking method obtains two lines including a colon centerline from the CT volume and a curved line representing the shape of a colonoscope (colonoscope line) from EM sensor outputs. The colon deforms by insertions of the colonoscope. A deformed colon centerline is calculated simulating the colon shape during colonoscope insertion. The CT and the sensor-coordinate systems are registered using the ICP algorithm. A transformation matrix between the two coordinate systems is obtained from a matching result of the deformed colon centerline and colonoscope line using the ICP algorithm. Five anatomical landmarks are detected on the colon centerline, deformed colon centerline, and colonoscope line. We find the colonoscope-tip position on the colon centerline using landmark-based coarse correspondence finding and length-based fine correspondence finding processes. These processes make correspondences between points on the deformed colon centerline
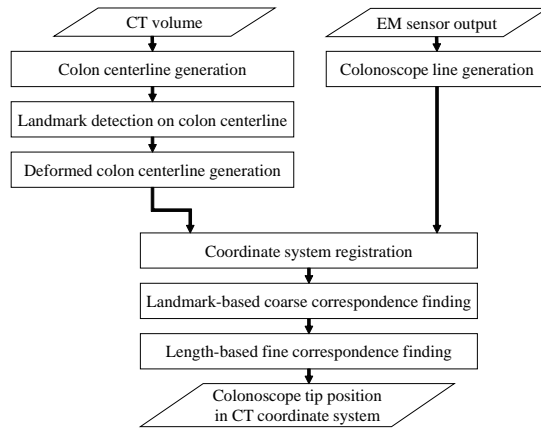
Fig. 1 Flowchart of the proposed method.

and points on the colonoscope line. The landmark-based coarse correspondence finding makes landmark pairs on the colon centerline and the colonoscope line. The length-based fine correspondence finding process finds the colonoscope-tip position on the colon centerline based on a ratio of line lengths between the landmarks. This process records line lengths of the colonoscope line. When the landmark-based coarse correspondence finding process fails to make correspondences with deformations of the colonoscope, the length-based fine correspondence finding process finds the colonoscope-tip position by using previously recorded line lengths. This makes the proposed method robust against deformations of the colon.

2.2 Colon centerline and colonoscope line generation

For the colon centerline generation, we utilize an abdominal CT volume taken in the distended state of the colon. A colonic-lumen region is extracted as an air region that has the largest volume in the body. A thinning process [17] is applied to the colonic-lumen region to obtain a thinned figure. The thinned figure has many spurious branches. We eliminate spurious branches by calculating the minimal path between the farthest two points on the thinned figure. To obtain a smoothed colon centerline, the cubic spline interpolation technique is utilized. We allocate control points at 20-mm intervals on the thinned figure. Then, a colon centerline is obtained using the cubic spline interpolation from the control points. The colon centerline generation process was originally proposed in [18]. The colon centerline is represented as a set of points $\mathbf{p}_i$ $(i = 1, \ldots, I)$ on the line. i and I are indexes of the points on the colon centerline and the number of points on the colon centerline. $\mathbf{p}_1$ and $\mathbf{p}_I$ are points at the anus and cecum. Figure 2 shows an example of a colon centerline of a colon phantom.
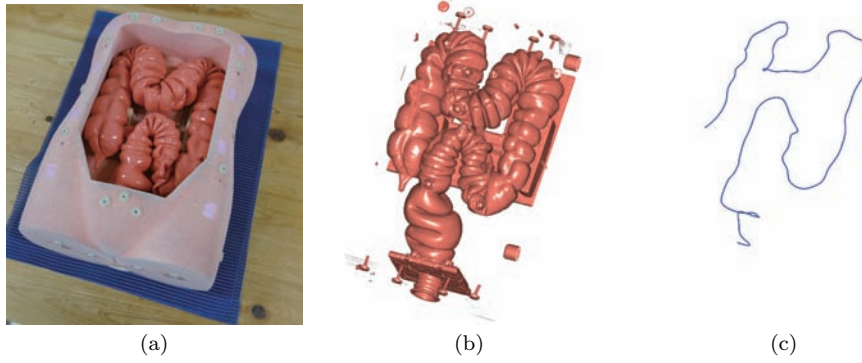
Fig. 2 (a) Colon phantom. (b) 3D-rendered image of phantom generated from CT volume. (c) Colon centerline of phantom.

For colonoscope-line generation, we utilize EM sensor outputs. We insert an Aurora 5/6DOF Shape Tool Type 1 (NDI, Ontario, Canada) in the colonoscope's working channel. The Aurora 5/6DOF Shape Tool Type 1 is equipped with seven EM sensors at 150-mm intervals. These sensors provide positions and tangent directions of the colonoscope tube at seven points. Let $\mathbf{s}_k$ and $\mathbf{m}_k$ $(k = 1, \ldots, 7)$ denote positions and directions obtained from the sensors. We apply the Hermite spline interpolation [19] to generate a smooth curve connecting the positions. The Hermite spline interpolation in the interval $(\mathbf{s}_k, \mathbf{s}_{k+1})$ is calculated as

$$\tilde{\mathbf{q}}_k(t) = h_{00}\mathbf{s}_k + h_{10}h\mathbf{m}_k + h_{01}\mathbf{s}_{k+1} + h_{11}h\mathbf{m}_{k+1}, \tag{1}$$

where $t \in [0, 1]$ and $h = ||\mathbf{s}_{k+1} - \mathbf{s}_k||$. The four Hermite basis functions are defined as

$$h_{00} = 2t^3 - 3t^2 + 1, \tag{2}$$
$$h_{10} = t^3 - 2t^2 + t, \tag{3}$$
$$h_{01} = -2t^3 + 3t^2, \tag{4}$$
$$h_{11} = t^3 - t^2. \tag{5}$$

We call the set of the Hermite spline interpolation curves in all intervals a colonoscope line. Points on the colonoscope line $\mathbf{q}_j$ $(j = 1, \ldots, J)$ are obtained from the Hermite spline interpolation curves. j and J are indexes of the points on the colonoscope line and the number of points on the colonoscope line. $\mathbf{q}_1$ is a point at the anus. Figure 3 shows the colon phantom with a colonoscope insertion and a colonoscope line.
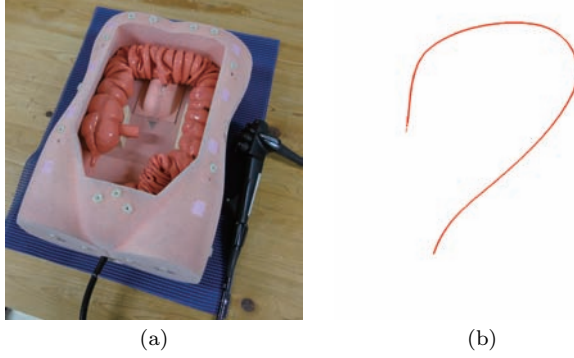
Fig. 3 (a) Colon phantom with colonoscope insertion. (b) Colonoscope line.

2.3 Landmark detection on colon centerline

We detect five landmarks on the colon centerline. The landmarks are points on the colon centerline that are close to the anus, the sigmoid/descending colon junction, the splenic flexure, the hepatic flexure, and the cecum. Indices of the points on the colon centerline at the landmarks are described as l_t^p ($t = 1, \ldots, 5$). t is the index of the landmarks. l_t^p satisfies the conditions

$$l_t^p \in 1, \ldots, I, \tag{6}$$

$$1 = l_1^p < l_2^p < l_3^p < l_4^p < l_5^p = I. \tag{7}$$

The landmarks on the colon centerline at the anus, the sigmoid/descending colon junction, the splenic flexure, the hepatic flexure, and the cecum are described as $\mathbf{p}_{l_1^p}, \ldots, \mathbf{p}_{l_5^p}$, respectively. Examples of a colon centerline and landmarks on it are shown in Fig. 4 (a). The following subsections provide details of the landmark detection method.
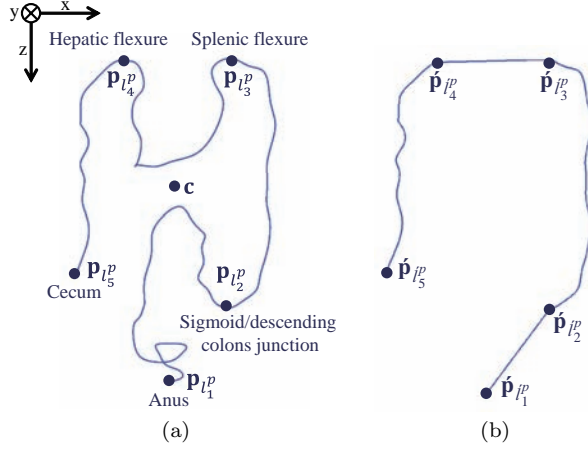
2.3.1 Anus and cecum

The end points of the colon centerline are defined as the landmarks at the anus and cecum. It is described as

$$\mathbf{p}_{l_1^p} = \mathbf{p}_1, \tag{8}$$

$$\mathbf{p}_{l_5^p} = \mathbf{p}_I. \tag{9}$$

2.3.2 Splenic flexure

The landmark at the splenic flexure $\mathbf{p}_{l_3^p}$ is selected as follows. The x- and z-axes run from the right-to-left and head-to-tail directions of the body, respectively.

Fig. 4 (a) A colon centerline and landmarks on it. (b) A deformed colon centerline and landmarks on it.

We define conditions

$$^{x}\mathbf{p}_{l_3^p} > {}^{x}\mathbf{c}, \tag{10}$$

$$^{z}\mathbf{p}_{l_3^p} < {}^{z}\mathbf{c}, \tag{11}$$

$$^{z}\mathbf{p}_{l_3^p} < {}^{z}\mathbf{p}_{l_3^p \pm 1}, \tag{12}$$

where $^{x}\mathbf{p}_{l_3^p}$ and $^{z}\mathbf{p}_{l_3^p}$ are the x- and the z-coordinates of $\mathbf{p}_{l_3^p}$. $\mathbf{c}$ is the median point of the CT volume. $^{x}\mathbf{c}$ and $^{z}\mathbf{c}$ are x- and z-coordinates of it. The conditions Eq. 10 and Eq. 11 mean $\mathbf{p}_{l_3^p}$ is located at the left- and head-side of the body. The condition Eq. 12 means the z-coordinate of $\mathbf{p}_{l_3^p}$ is the local minimum. Among points satisfying the conditions Eq. 10, 11, and 12, the most distant point from $\mathbf{c}$ is defined as $\mathbf{p}_{l_3^p}$.

2.3.3 Hepatic flexure

The landmark at the hepatic flexure $\mathbf{p}_{l_4^p}$ is selected as follows. We define conditions

$$^{x}\mathbf{p}_{l_4^p} < {}^{x}\mathbf{c}, \tag{13}$$

$$^{z}\mathbf{p}_{l_4^p} < {}^{z}\mathbf{c}, \tag{14}$$

$$^{z}\mathbf{p}_{l_4^p} < {}^{z}\mathbf{p}_{l_4^p \pm 1}. \tag{15}$$

The superscripts x and z mean x- and z-coordinates. The conditions Eq. 13 and Eq. 14 mean $\mathbf{p}_{l_4^p}$ is located at the right- and head-side of the body. The condition Eq. 15 means the z-coordinate of $\mathbf{p}_{l_4^p}$ is the local minimum. Among points satisfying the conditions Eq. 13, 14, and 15, the most distant point from $\mathbf{c}$ is defined as $\mathbf{p}_{l_4^p}$.

2.3.4 Sigmoid/descending colon junction

The landmark at the sigmoid/descending colon junction $\mathbf{p}_{l_2^p}$ is selected as follows. We define conditions

$$^z\mathbf{p}_{l_2^p} > {}^z\mathbf{p}_{l_2^p \pm 1}, \tag{16}$$

$$^z\mathbf{p}_{l_2^p} > {}^z\mathbf{p}_{S_1}, \tag{17}$$

$$^z\mathbf{p}_{l_2^p} > {}^z\mathbf{p}_{S_2}, \tag{18}$$

$$\sum_{i=l_1^p}^{l_2^p-1} ||\mathbf{p}_{i+1} - \mathbf{p}_i|| > \frac{\sum_{i=l_1^p}^{l_3^p-1} ||\mathbf{p}_{i+1} - \mathbf{p}_i||}{3}, \tag{19}$$

$$\sum_{i=l_2^p}^{l_3^p-1} ||\mathbf{p}_{i+1} - \mathbf{p}_i|| > \frac{\sum_{i=l_1^p}^{l_3^p-1} ||\mathbf{p}_{i+1} - \mathbf{p}_i||}{3}. \tag{20}$$

Again, the superscript z means z-coordinate. S_1 is the maximum value of the index of the colon centerline, which satisfies

$$S_1 < l_2^p, \tag{21}$$

$$D \le \sum_{i=S_1}^{l_2^p-1} ||\mathbf{p}_{i+1} - \mathbf{p}_i||, \tag{22}$$

where D mm is a threshold of distance along the colon centerline. S_2 is the minimum value of the index of the colon centerline, which satisfies

$$S_2 > l_2^p, \tag{23}$$

$$D \le \sum_{i=l_2^p}^{S_2-1} ||\mathbf{p}_{i+1} - \mathbf{p}_i||. \tag{24}$$

The conditions Eqs. 16, 17, and 18 mean the z-coordinate of $\mathbf{p}_{l_2^p}$ is the local maximum in consideration of the neighboring points and points D mm away from $\mathbf{p}_{l_2^p}$. The conditions Eq. 19 and 20 mean $\mathbf{p}_{l_2^p}$ is distant from both $\mathbf{p}_{l_1^p}$ and $\mathbf{p}_{l_3^p}$. Among points satisfying the conditions Eq. 16, 17, 18, 19 and 20, a point $\mathbf{p}_{l_2^p}$ that maximizes

$$(^z\mathbf{p}_{l_2^p} - {}^z\mathbf{p}_{S_1}) + (^z\mathbf{p}_{l_2^p} - {}^z\mathbf{p}_{S_2}), \tag{25}$$

is defined as the landmark at the sigmoid/descending colon junction.

2.4 Deformed colon centerline generation

The colon centerline and colonoscope line are registered in the coordinate registration process to find a transformation matrix between the CT and sensor coordinate systems. However, the shapes of two lines largely differ because

colonoscope insertion deforms the colon. During colonoscope insertion, the transverse and sigmoid colons are straightened. We generate a deformed colon centerline, which has a similar shape to the colonoscope line, by partly changing the shape of the colon centerline. The deformed colon centerline is generated by replacing points on the colon centerline in the rectum/sigmoid and transverse colon areas with points on straight-line sections. The points on the colon centerline in the rectum/sigmoid colon area are defined as points that have index $l_1^p, \ldots, l_2^p$. Also, the points on the colon centerline in the transverse colon area are defined as points that have index $l_3^p, \ldots, l_4^p$.

The deformed colon centerline is a set of points $\acute{\mathbf{p}}_{\acute{i}}$ ($\acute{i} = 1, \ldots, \acute{I}$). Five landmarks are defined on the deformed colon centerline similarly to the colon centerline. Indices of the points on the deformed colon centerline at the landmarks are $\acute{l}_t^p$. The $\acute{l}_t^p$ satisfies the conditions

$$\acute{l}_t^p \in 1, \ldots, \acute{I}, \tag{26}$$

$$1 = \acute{l}_1^p < \acute{l}_2^p < \acute{l}_3^p < \acute{l}_4^p < \acute{l}_5^p = \acute{I}. \tag{27}$$

The landmarks on the deformed colon centerline at the anus, sigmoid/descending colon junction, splenic flexure, hepatic flexure, and cecum are described as $\acute{\mathbf{p}}_{\acute{l}_1^p}, \ldots, \acute{\mathbf{p}}_{\acute{l}_5^p}$, respectively. Examples of a deformed colon centerline and landmarks on it are shown in Fig. 4 (b).

Points of the landmarks on the deformed colon centerline are set as

$$\acute{\mathbf{p}}_{\acute{l}_1^p} = \mathbf{p}_{l_1^p}, \quad \text{where} \quad \acute{l}_1^p = l_1^p = 1, \tag{28}$$

$$\acute{\mathbf{p}}_{\acute{l}_2^p} = \mathbf{p}_{l_2^p}, \quad \text{where} \quad \acute{l}_2^p = h, \tag{29}$$

$$\acute{\mathbf{p}}_{\acute{l}_3^p} = \mathbf{p}_{l_3^p}, \quad \text{where} \quad \acute{l}_3^p = h + (l_3^p - l_2^p), \tag{30}$$

$$\acute{\mathbf{p}}_{\acute{l}_4^p} = \mathbf{p}_{l_4^p}, \quad \text{where} \quad \acute{l}_4^p = \acute{l}_3^p + h = 2h + (l_3^p - l_2^p), \tag{31}$$

$$\acute{\mathbf{p}}_{\acute{l}_5^p} = \mathbf{p}_{l_5^p}, \quad \text{where} \quad \acute{l}_5^p = \acute{l}_4^p + (l_5^p - l_4^p) = 2h + (l_3^p - l_2^p) + (l_5^p - l_4^p), \tag{32}$$

where h is the number of points on the straight-line section.

Points on the deformed colon centerline are calculated by

$$\acute{\mathbf{p}}_{\acute{i}} = \begin{cases} \left(1 - \frac{\acute{i} - \acute{l}_1^p}{h}\right) \mathbf{p}'_{\acute{l}_1^p} + \left(\frac{\acute{i} - \acute{l}_1^p}{h}\right) \acute{\mathbf{p}}_{\acute{l}_2^p}, & \text{if } \acute{i} = \acute{l}_1^p, \ldots, \acute{l}_2^p, \\ \mathbf{p}_{\acute{i} - \acute{l}_2^p + l_2^p}, & \text{if } \acute{i} = \acute{l}_2^p, \ldots, \acute{l}_3^p, \\ \left(1 - \frac{\acute{i} - \acute{l}_3^p}{h}\right) \mathbf{p}'_{\acute{l}_3^p} + \left(\frac{\acute{i} - \acute{l}_3^p}{h}\right) \acute{\mathbf{p}}_{\acute{l}_4^p}, & \text{if } \acute{i} = \acute{l}_3^p, \ldots, \acute{l}_4^p, \\ \mathbf{p}_{\acute{i} - \acute{l}_4^p + l_4^p}, & \text{if } \acute{i} = \acute{l}_4^p, \ldots, \acute{l}_5^p. \end{cases} \tag{33}$$

2.5 Coordinate system registration

In colonoscopic examinations, observations of the colon and treatments are performed while pulling back the colonoscope after its insertion up to the cecum. We assume the colonoscope-tip is inserted up to the cecum when this

coordinate system registration process is applied. This process is applied only once before the processes described in sections 2.6 and 2.7 are performed.

Points on the deformed colon centerline $\acute{\mathbf{p}}_i$ and the colonoscope line $\mathbf{q}_j$ are in the CT and sensor coordinate systems, respectively. We register these two coordinate systems using the ICP algorithm [20].

The ICP algorithm finds a rigid transformation matrix between the two point sets $\acute{\mathbf{p}}_i$ and $\mathbf{q}_j$ by minimizing Euclidean distances between the two point sets. In this registration, we fix correspondences between a pair $\acute{\mathbf{p}}_{\acute{1}}$ and $\mathbf{q}_1$, and a pair $\acute{\mathbf{p}}_{\acute{I}}$ and $\mathbf{q}_J$.

2.6 Landmark-based coarse correspondence finding

We apply the transformation matrix obtained in section 2.5 to $\mathbf{q}_j$ to calculate points on the colonoscope line in the CT coordinate system $^c\mathbf{q}_j$. This process is applied every time the colonoscope line changes.

We detect five landmarks on the colonoscope line in the CT coordinate system. The landmarks are points on the colonoscope line in the CT coordinate system that are closest to the landmarks on the deformed colon centerline. Indices of the points on the colonoscope line in the CT coordinate system at the landmarks are described as l_t^q. l_t^q satisfies the conditions

$$l_t^q \in 1, \ldots, J \cup \{null\}, \tag{34}$$

where $\{null\}$ means the situation that the landmark is not detected. The landmarks on the colonoscope line in the CT coordinate system are described as $^c\mathbf{q}_{l_1^q}, \ldots, ^c\mathbf{q}_{l_5^q}$.

We assume $^c\mathbf{q}_1$ is located near the anus. We define the index value of the landmark on the colonoscope line in the CT coordinate system at the anus as $l_1^q = 1$. For $t = 2, \ldots 5$, the indices of the landmarks on the colonoscope line in the CT coordinate system are obtained by

$$l_t^q = \begin{cases} \arg\min_j ||^c\mathbf{q}_j - \acute{\mathbf{p}}_{\acute{l}_t^p}||, & \text{if} \quad ||^c\mathbf{q}_j - \acute{\mathbf{p}}_{\acute{l}_t^p}|| \leq R, \\ \{null\}, & \text{otherwise}, \end{cases} \tag{35}$$

where R is a threshold of correspondence finding between the landmarks on the colonoscope line in the CT coordinate system and deformed colon centerline. Figure 5 shows examples of landmarks on a colonoscope line. Correspondences between the landmarks on the deformed colon centerline and the colonoscope line in the CT coordinate system can be established from results obtained in this section.

2.7 Colonoscope-tip position detection by length-based fine correspondence finding

In this process, we find a position on the deformed colon centerline that corresponds to the colonoscope-tip position. A position on the colon centerline
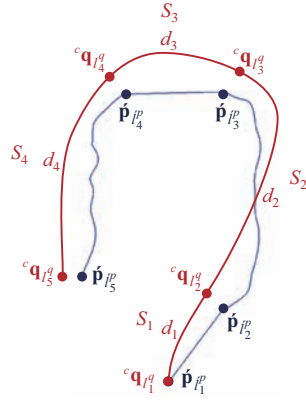
Fig. 5 Examples of landmarks on a colonoscope line. The red and blue lines represent a colonoscope line and a deformed colon centerline. $S_1, \ldots, S_4$ are segments of the colonoscope line. $d_1, \ldots, d_4$ are lengths along the colonoscope line in the segments.

that corresponds to the colonoscope-tip is easily obtained from the relationship between the colon centerline and deformed colon centerline. This process is applied every time the colonoscope line changes.

We define segments S_a ($a = 1, \ldots, 4$), which consist of the points on the colonoscope line in the CT coordinate system. The segments $S_1, \ldots, S_4$ correspond to the rectum/sigmoid, descending, transverse, and ascending colon areas, respectively. Points on the colonoscope line in the CT coordinate system that have index $l_1^q, \ldots, l_2^q - 1$ are included in the segment of the rectum/sigmoid colon area S_1. Similarly, $\mathbf{q}_{l_2^q}, \ldots, \mathbf{q}_{l_3^q - 1} \in S_2$, $\mathbf{q}_{l_3^q}, \ldots, \mathbf{q}_{l_4^q - 1} \in S_3$, and $\mathbf{q}_{l_4^q}, \ldots, \mathbf{q}_{l_5^q} \in S_4$. Examples of the segments are shown in Fig. 5.

We define the length along the colonoscope line in the CT coordinate system between the landmarks as d_a. d_1 is the length from ${}^c\mathbf{q}_{l_1^q}$ to ${}^c\mathbf{q}_{l_2^q}$, d_2 is the length from ${}^c\mathbf{q}_{l_2^q}$ to ${}^c\mathbf{q}_{l_3^q}$, d_3 is the length from ${}^c\mathbf{q}_{l_3^q}$ to ${}^c\mathbf{q}_{l_4^q}$, and d_4 is the length from ${}^c\mathbf{q}_{l_4^q}$ to ${}^c\mathbf{q}_{l_5^q}$. A schematic illustration of the lengths is shown in Fig. 5. The value d_a is updated when landmarks of both ends of the segment S_a are detected ($l_a^q, l_{a+1}^q \neq \{null\}$).

One end of the colonoscope line in the CT coordinate system ${}^c\mathbf{q}_J$ corresponds to the colonoscope-tip position. The position of ${}^c\mathbf{q}_J$ is either on one of the landmarks (Fig. 6 (a)) or included in one of the segments S_a (Fig. 6 (b), (c)). The following processes are applied to find a position on the deformed colon centerline that corresponds to the colonoscope-tip position.

When the index of the colonoscope-tip position satisfies $l_t^q = J$, which means the colonoscope-tip position ${}^c\mathbf{q}_J$ corresponds to one of the landmarks (Fig. 6 (a)). A position on the deformed colon centerline that corresponds to the colonoscope-tip position is a landmark $\acute{\mathbf{p}}_{l_t^p}$.

When the colonoscope-tip position $^c\mathbf{q}_J$ is included in one of the segments S_a, any one of the following processes is applied.

Case 1 Colonoscope-tip position is in a segment with a detected landmark:
This process is applied if the colonoscope-tip position $^c\mathbf{q}_J$ is in a segment S_a, and a landmark at an end of the segment is detected ($l_a^q \neq \{null\}$) (Fig. 6 (b)). A position on the deformed colon centerline that corresponds to the colonoscope-tip position is $\acute{\mathbf{p}}_{n^\alpha}$. n^α is defined based on a ratio of the length along the colonoscope line in the CT coordinate system to the length along the deformed colon centerline in S_a. n^α is calculated by

$$n^\alpha = \acute{l}_a^p + (\acute{l}_{a+1}^p - \acute{l}_a^p)\frac{d^\alpha}{d_a}, \tag{36}$$

where d^α is a length along the colonoscope line in the CT coordinate system from $^c\mathbf{q}_J$ to $^c\mathbf{q}_{l_a^q}$.

Case 2 Colonoscope-tip position is in a segment without detected landmark:
This process is applied if the colonoscope-tip position $^c\mathbf{q}_J$ is in a segment S_a, and a landmark at an end of the segment is not detected ($l_a^q = \{null\}$) (Fig. 6 (c)). A position on the deformed colon centerline that corresponds to the colonoscope-tip position is $\acute{\mathbf{p}}_{n^\beta}$. n^β is defined based on a ratio of the length along the colonoscope line in the CT-coordinate system to the length along the deformed colon centerline in S_a and S_{a-1}. n^β is calculated by

$$n^\beta = \acute{l}_{a-1}^p + (\acute{l}_{a+1}^p - \acute{l}_{a-1}^p)\frac{d^\beta}{d_a + d_{a-1}}, \tag{37}$$

where d^β is a length along the colonoscope line in the CT-coordinate system from $^c\mathbf{q}_J$ to $^c\mathbf{q}_{l_{a-1}^q}$.

We obtain the position on the colon centerline that corresponds to the colonoscope-tip as described above. The position can be utilized to show the colonoscope-tip position in the colon or navigate a physician to desired positions.

3 Experiments

3.1 Landmark detection on colon centerline

We evaluated the landmark detection accuracy of the landmark detection method on the colon centerline 2.3 using ten cases of abdominal CT volumes of real patients. The CT volumes were taken in a distended state of the colon. The acquisition parameters of the CT volumes are; image size: 512×512 pixles, slice number: 349–818, pixel spacing: 0.54–0.78 mm, slice spacing: 0.50–1.25 mm, and slice thickness: 0.50–2.50 mm. The detection results were visually confirmed by an engineering researcher. The colon shapes and landmark detection results are shown in Fig. 7.
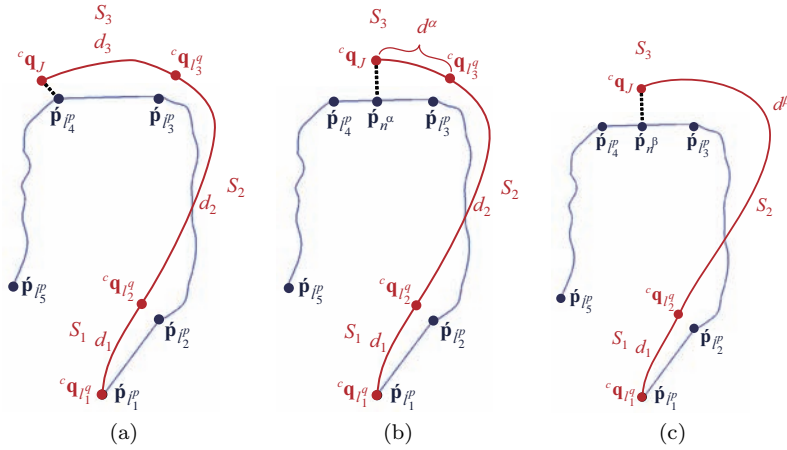
Fig. 6 Positional relationships of deformed colon centerlines (blue lines) and colonoscope lines (red lines): (a) a colonoscope-tip position on a landmark, (b) a colonoscope-tip position in a segment with a detected landmark, and (c) a colonoscope-tip position in a segment without detected landmark.

The anus and cecum landmarks were correctly detected in all cases because they are the end points of the colon centerline. Also, the hepatic and sigmoid/descending colon junction landmarks were correctly detected in all cases. The splenic flexure landmarks were correctly detected in eight cases. In the rest of two cases, the splenic flexure landmarks were detected on the transverse colon (Fig. 7 (h)). All landmarks were correctly detected in Fig. 7 (b), (d), and (f).

3.2 Colonoscope tracking

We evaluated the accuracy of the proposed colonoscope-tracking method. We used a colon phantom (Colonoscopy training model type I-B, Koken, Tokyo, Japan) and a colonoscope (CF-Q260AI, Olympus, Tokyo, Japan) to simulate colonoscope insertions to the colon. A CT volume of the phantom was taken and utilized in the experiments. The phantom is made of silicone rubber. The phantom is designed for trainings of colonoscope insertions for physicians. The shape and deformability of it is similar to those of real colons. The dimensions of the phantom is given in Fig. 8 (a). The diameter of the colon of it is about 5 cm. An Aurora 5/6DOF Shape Tool Type 1 (NDI, Ontario, Canada) was used to obtain colonoscope lines. The Aurora 5/6DOF Shape Tool Type 1 was equipped with seven EM sensors at 150-mm intervals. Accuracies of the EM sensors are 0.48 mm RMS error for a EM sensor at the Aurora 5/6DOF Shape Tool Type 1 tip and 0.70 mm RMS error for the other EM sensors. It is inserted in the colonoscope's working channel. The Aurora 5/6DOF Shape Tool Type 1 is flexible. Thus, it gave no influence to the movement of the colonoscope. We
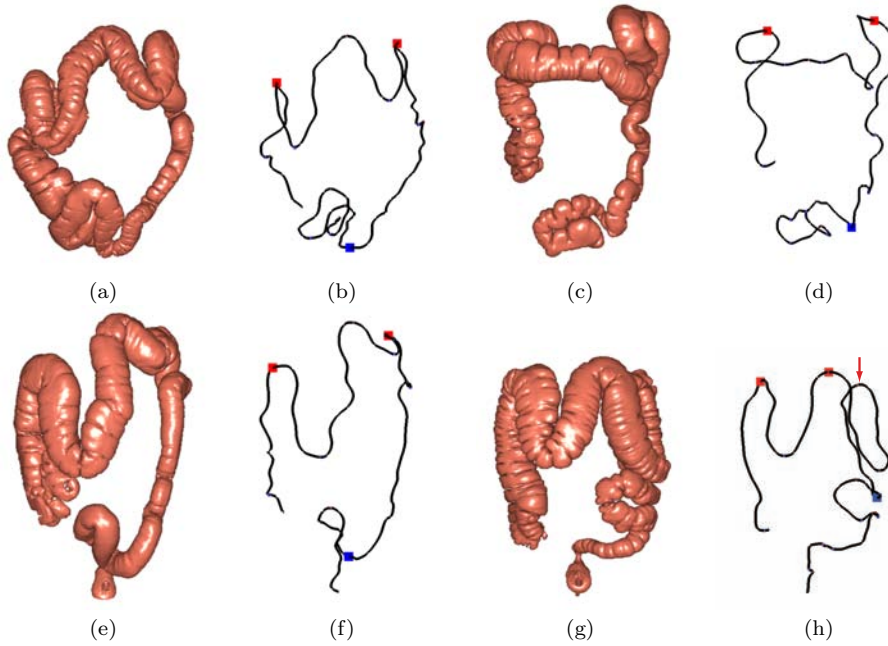
Fig. 7 Colon shapes and landmark detection results. (a), (c), (e), and (g) are colon shapes. (b), (d), (f), and (h) are corresponding landmark detection results. Red and blue points indicate landmarks. Correct landmarks were obtained in (b), (d), and (f). All landmarks were correctly detected in (b), (d), and (f). The splenic flexure landmark was detected on the transverse colon in (h). Correct splenic flexure landmark position is indicated by an arrow.

fixed the Aurora 5/6DOF Shape Tool Type 1 to the colonoscope at the working channel port of the colonoscope. By the fixing, the the Aurora 5/6DOF Shape Tool Type 1 keeps the same position in the colonoscope. The parameter of the method was set as $D = 50$ mm. Setting of the parameter R is described later.

We utilized tracking error as a criterion of performance evaluation of the proposed method. 15 markers were defined on the surface of the colon phantom, which can be observed in the CT volume (Fig. 8 (b)). Positions of the markers were: (M1–M3) the ascending colon, (M4) a position near the hepatic flexure, (M5–M7) the transverse colon, (M8) a position near the splenic flexure, (M9–M11) the descending colon, (M12) a position near the junction of the sigmoid/descending colons, and (M13–M15) the sigmoid colon and rectum. The tracking error is defined as follows. Positions of the markers were projected to the colon centerline. The tracking error is the length along the colon centerline from an estimated position of the colonoscope-tip to a position of a projected marker, when the colonoscope-tip comes closest to the marker.

In colonoscopic examinations, physicians insert the colonoscope-tip up to the cecum. Physicians do not try to find lesions while the insertion because the colonoscope is used to push the colonic wall and views of the colonoscope
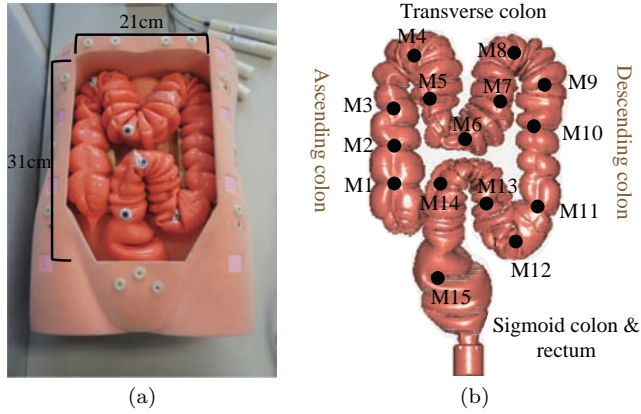
Fig. 8 (a) The dimensions of a colon phantom and (b) positions of markers on the surface of a colon phantom.

are blocked often. After colonoscope insertion up to the cecum, physicians observe the colonic wall while pulling back the colonoscope. The proposed method tracks the colonoscope-tip position while colonic wall observations. Based on the colonoscopic examination method, we performed tracking error measurements as follows. In measurement of the tracking errors, we first insert the colonoscope-tip up to the cecum to perform the coordinate system registration. The shapes of the transverse and sigmoid colons were changed from bended to straighten by the insertion of the colonoscope. The shapes of the ascending and descending colons were not changed by the insertion. After performing the coordinate system registration, the landmark detection on the colonoscope line in the CT coordinate system and the colonoscope-tip position detection processes are applied to find the colonoscope-tip position. These two processes were continuously applied while pulling back the colonoscope. The tracking errors were measured while pulling back the colonoscope. After the colonoscope-tip passes through the transverse and sigmoid colons, they restored their original shapes.

To evaluate tracking performance of the proposed method, we measured tracking errors in five trials of colonoscope insertion. The parameter R is the threshold of correspondence finding between the landmarks on the colonoscope line in the CT coordinate system and deformed colon centerline. Detection results of the landmark on the colonoscope line in the CT coordinate system are affected by the value setting of R. To check their relationships, we measured tracking errors in value settings $R = 10, 20, 30$, and 40 mm. Tracking error measurement results are shown in Fig. 9. We counted the number of failure of landmark detection on the colonoscope line during colonoscope insertions. Average numbers of landmark detection failures per one colonoscope insertion are shown in Table 1.
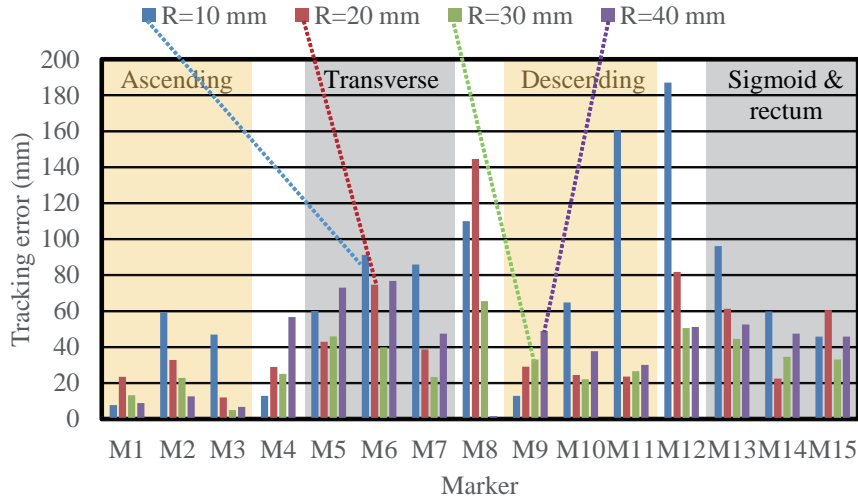
Fig. 9 Average tracking errors at each marker for $R = 10, 20, 30, 40$ mm.

Table 1 Average number of landmark detection failures per one colonoscope insertion for $R = 10, 20, 30, 40$ mm.

	R mm			
	10	20	30	40
Average number	3.4	2.4	0.8	0

We measured processing time of the proposed method. We performed tracking of the colonoscope from the cecum to anus five times. A Windows 10 PC with an Intel Core i7-4930MX 3.2GHz CPU and 32GB RAM was used in this experiment. The average processing time was 0.19 sec. per frame.

4 Discussion

4.1 Landmark detection on colon centerline

We applied the colonoscope tracking method to tracking in the colon phantom. The tracking method have potential to perform tracking in real patients. To show this potential, we applied the landmark detection method on the colon centerline. Correct landmark detection results contribute accurate colonoscope tracking. From the results shown in section 3.1, the landmark detection method correctly detected most of landmarks. Though the colon has large variation in the shape, the landmark detection method specified correct landmark positions. This results show our colonoscope tracking method have potential to perform tracking in real patients.

The splenic flexure landmark was detected at wrong positions in two cases. In these cases, the transverse colon made curved shape that shows similar shape to curve at the splenic flexure. The condition of the splenic flexure landmark detection (section 2.3.2) needs to be updated to obtain better results.

4.2 Colonoscope tracking

We performed colonoscope tracking utilizing a CT volume and EM sensors. The proposed method makes it possible to track the colonoscope-tip position in the full length of the colon in real time. Furthermore, the proposed method requires minimal manual interactions. The advance preparation of the proposed method to perform tracking is quite simple. The proposed method automatically generate a colon centerline from a CT volume. The coordinate system registration is also automated. It does not require any manual specification of corresponding points between the coordinate systems. While performing a colonoscope tracking, the proposed method automatically shows estimated position without any manual interaction to the method. This helps physicians concentrate on colonoscope operations. Unlike the image-based colonoscope tracking method [11], the proposed method keeps tracking even if unclear colonoscopic images are observed. Furthermore, the proposed method is designed to track the colonoscope-tip position under large deformations of the colon or colonoscope. The proposed method tracked the colonoscope-tip position even if detection of the landmark on the colonoscope line failed to detect a landmark. The colon is largely deformed during colonoscopic examinations with insertion of the colonoscope. The colonoscope also deforms during the examinations. The colonoscope-tip position detection process is made to find the colonoscope-tip position if the landmark detection on the colonoscope line fails. This process makes the proposed method robust against deformations of the colon. The proposed method is applicable to navigation systems of the colonoscope.

The image-based colonoscope tracking method proposed by Liu et al. [11] was evaluated using phantoms and real colonoscope image sequences. In their phantom study, displacement error was under 7 mm. However, their phantoms were rigid and have quite simple shapes (straight and curve shapes). The phantoms have characteristic texture patterns inside of them to help image-based tracking. Their phantoms have quite different shape, texture, and deformation property from the colon. They also performed real colonoscope image study. They performed colonoscope tracking only in limited sequences in the colon. Their method failed to track when the colonoscope quickly moves. Our method can track full length of the colon from the cecum to anus continuously. Also, our method keeps tracking even if the colonoscope quickly moves. Sensor-based colonoscopy guiding methods [12,13] have been proposed. They are colonoscope shape calculation method without utilization of information related to the colon. They cannot estimate the colonoscope-tip position in

the colon. Our method estimates the colonoscope-tip position by combining information from sensors and the CT volume.

The bronchoscope tracking methods are related to the proposed method. Their purpose is the estimation of the endoscope-tip position in the hollow organ (the trachea and bronchi), which is similar to the proposed method. Our research team has been working on bronchoscope tracking since 2001. Bronchoscope tracking methods are mainly classified into three categories: (a) image-based matching [4–6], (b) EM-sensor based tracking [7,8], and (c) hybrid one [9,10]. The method (a) cannot be used for the purpose of colonoscope tracking because the colonoscope cannot capture specific structures such as bifurcations of branches. In bronchoscope tracking, even if the system fails in tracking, the tracking recovers around bifurcations. However, such structures are missing in the colon. (b) EM-sensor based tracking is also utilized for bronchoscope. One method is fiducial based tracking. The other is center-line registration. This registration method registers the insertion path of the bronchoscope with the centerlines of branches. Since the bronchus has tree structure that have branches defining space, branch centerline and insertion path registration work well. This cannot be applied to the colon. Although bronchi show some deformations due to endoscope insertion, overall shape deformation is not big if you compare with deformation of the colon. This makes difficult to utilize the bronchoscope tracking method to the colonscope tracking. Our method continue tracking even if large deformation of the colon occurs. Our method is most suitable for the colonoscope tracking.

The tracking errors of the proposed method were smaller than 50 mm at most of markers when we set $R = 30$ or 40 mm. A physician who specializes in gastroenterology gave a comment that tracking errors smaller than 50 mm are acceptable for colonoscope navigation to positions of polyps. This is because polyps are observable from the colonoscope camera when positions of the colonoscope-tip and polyps are closer than 50 mm. Summers et al. [2] showed a criterion that is similar to the tracking error. They detected polyps in CT volumes and confirmed the polyp positions in the real patient bodies by using a colonoscope. They calculated positional errors between detected polyps in CT volumes and real-patient bodies. The positional error is similar to the tracking error. In their results, positional errors within 100 mm were considered as good results. The proposed method can satisfy tracking errors smaller than 100 mm. From these results, the proposed method has potential to allow colonoscope tracking in clinical fields if all of the landmarks on the colonoscope line are detected.

The number of failures of landmark detection on the colonoscope line (Table 1) have relationship to the tracking errors. When we set $R = 30$ or 40 mm, both of the landmark detection failure numbers and tracking errors were small. In this case, the Case 1 condition in the colonoscope-tip position detection (shown in section 2.7) was used in the tracking. The colonoscope-tip position detection calculated accurate results using landmark detection results at all landmarks. When we set $R = 20$ mm, the landmark detection failure occurred 2.4 times per a colonoscope insertion. Detection of the splenic flex-

ure landmark on the colonoscope line failed every colonoscope insertions. This detection failure resulted in the increase of tracking error at M8 marker. In our experiments, distance between the colon centerline and colonoscope line at the splenic flexure landmark was large because of the colon and colonoscope deformations. When we set $R = 10$ mm, the number of landmark detection failure increased compared to the other parameter settings. In addition to the splenic flexure landmark detection failure, the sigmoid/descending colon junction landmark detection failed every colonoscope insertions. Large tracking errors were observed around M8 and M12 markers. The parameter setting $R = 10$ mm was severe setting in the landmark detection on the colonoscope line. It increased both of the number of landmark detection failure and the tracking errors. To improve our method, value of the parameter R should be changed based on positions in the colon or colonoscope insertion conditions.

Limitations of the proposed method can be summarized as follows. First, the proposed method depends on the detection accuracy of landmark points. Although our phantom test showed good performance in detection of landmarks, only one physical phantom is utilized in this paper. Further work testing landmark detection should be conducted. Second, the proposed method shows deteriorated performance in endoscope tracking in greatly deformed areas including the sigmoid colon. Some combination with image-based tracking method is necessary for improving tracking performance. Third, only one physical phantom was utilized here. It is difficult to obtain other phantoms commercially. Construction of phantoms and their utilization for testing remains as our future work. Fourth, the proposed method is evaluated in the theoretical idealized experiments. Evaluation in more realistic settings is included in our future work. Human testing also remains as future work with IRB approval.

5 Conclusions

This paper proposed a colonoscope-tracking method robust for deformations of the colon. The proposed method generates the colon centerline and the colonoscope line. The colon centerline is deformed to simulate the deformed shape of the colon during colonoscope insertions. Five anatomical landmarks are detected on the two lines. After applying the coordinate system registration, the colonoscope-tip position is calculated based on the length along the lines between the landmarks. The proposed method keeps tracking when the colon and colonoscope shapes deform by utilizing previously obtained line lengths. Experimental results using the colon phantom showed that the proposed method finds the colonoscope-tip position with tracking errors smaller than 50 mm in most trials, when all of the landmarks on the colonoscope line were detected. The tracking errors increased when no landmark was detected. Future work includes optimal parameter finding, modelization of colon deformations, and utilization of colonoscopic images for colonoscope tracking.

References

1. Yoshida H (2005) Three-dimensional computer-aided diagnosis in CT colonography. Multidimensional Image Processing, Analysis, and Display: RSNA Categorical Course in Diagnostic Radiology Physics:237–251
2. Summers RM, Swift JA, Dwyer AJ, Choi R, Pickhardt PJ (2009) Normalized Distance Along the Colon Centerline: A Method for Correlating Polyp Location on CT Colonography and Optical Colonoscopy. American Journal of Roentgenology 193(5):1296–1304
3. Peters T, Cleary K (2008) Image-Guided Interventions: Technology and Applications. Springer, Germany
4. Deligianni F, Chung A, Yang GZ (2005) Predictive camera tracking for bronchoscope simulation with condensation. Proceedings of MICCAI 3749:910–916
5. Rai L, Helferty JP, Higgins WE (2008) Combined video tracking and image-video registration for continuous bronchoscopic guidance. International Journal of Computer Assisted Radiology and Surgery 3:3–4
6. Deguchi D, Mori K, Feuerstein M, Kitasaka T, Maurer Jr CR, Suenaga Y, Takabatake H, Mori M, Natori H (2009) Selective image similarity measure for bronchoscope tracking based on image registration. Medical Image Analysis 3(14):621–633
7. Gildea TR, Mazzone PJ, Karnak D, Meziane M, Mehta A (2006) Electromagnetic navigation diagnostic bronchoscopy: a prospective study. American Journal of Respiratory and Critical Care Medicine 174(9):982–989
8. Schwarz Y, Greif J, Becker H, Ernst A, Metha A (2006) Real-time electromagnetic navigation bronchoscopy to peripheral lung lesions using overlaid CT images: the first human study. Chest 129(4):988–994
9. Mori K, Deguchi D, Akiyama K, Kitasaka T, Mauler Jr CR, Suenaga Y, Takabatake H, Mori M, Natori H (2005) Hybrid bronchoscope tracking using a magnetic tracking sensor and image registration. Medical Image Computing and Computer-Assisted Intervention (MICCAI) 3750:543–550
10. Luo X, Wan Y, He X, Mori K (2015) Observation-driven adaptive differential evolution and its application to accurate and smooth bronchoscope three-dimensional motion tracking. Medical Image Analysis 24:282–296
11. Liu J, Subramanian KR, Yoo TS (2013) An optical flow approach to tracking colonoscopy video. Computerized Medical Imaging and Graphics 37(3):207–223
12. Ching LY, Moller K, Non-radiological colonoscope tracking image guided colonoscopy using commercially available electromagnetic tracking system (2010) IEEE Conference on Robotics Automation and Mechatronics (RAM):62–67
13. Fukuzawa M, Uematsu J, Kono S, Suzuki S, Sato T, Yagi N, Tsuji Y, Yagi K, Kusano C, Gotoda T, Kawai T, Moriyasu F, Clinical impact of endoscopy position detection unit (UPD-3) for a non-sedated colonoscopy (2015) World Journal of Gastroenterology 21(16):4903–4910
14. Oda M, Acar B, Furukawa K, Kitasaka T, Suenaga Y, Navab N, Mori K, Colonoscope tracking method based on line registration using CT images and electromagnetic sensors (2013) International Journal of Computer Assisted Radiology and Surgery 8(1):S349–S351
15. Oda M, Kondo H, Kitasaka T, Furukawa K, Miyahara R, Hirooka Y, Goto H, Navab N, Mori K, Colonoscope navigation system using colonoscope tracking method based on line registration (2014) Proceedings of SPIE 9036:903626-1–7
16. Kondo H, Oda M, Furukawa K, Miyahara R, Hirooka Y, Goto H, Kitasaka T, Mori K, Development of marker-free estimation method of colonoscope tip position using electromagnetic sensors and CT volumes (2014) International Journal of Computer Assisted Radiology and Surgery 9(1):S11–S12

17. Saito T, Toriwaki J, A sequential thinning algorithm for three dimensional digital pictures using the Euclidean distance transformation (1995) Proceedings of 9th SCIA (Scandinavian Conference on Image Analysis):507–516
18. Oda M, Hayashi Y, Kitasaka T, Mori K, Suenaga Y, A method for generating virtual unfolded view of colon using spring model (2006) Proceedings of SPIE 6143:61431C-1–12
19. Chen ECS, Fowler SA, Hookey LC, Ellis RE, Representing flexible endoscope shapes with Hermite splines (2010) Proceedings of SPIE 7625:76251D-1–7
20. Besl PJ, McKay ND (1992) A method for registration of 3-D shapes. IEEE Transactions on Pattern Analysis and Machine Intelligence 14:239–256